CATÓLICA
FACULDADE DE MEDICINA DENTÁRIA
VISEU

EFFECTS OF COLOR AND SPECIAL GEOMETRIC FORMS ON SCAN SPEED AND TRUENESS OF COMPLETE ARCH DIGITAL IMPLANT SCANS USING TRIOS 4

Dissertação apresentada à Universidade Católica Portuguesa
para obtenção do grau de Mestre em Medicina Dentária

Ana Lia Almeida Mendes

Viseu, 2025

CATÓLICA
FACULDADE DE MEDICINA DENTÁRIA
VISEU

EFFECTS OF COLOR AND SPECIAL GEOMETRIC FORMS ON SCAN SPEED AND TRUENESS OF COMPLETE ARCH DIGITAL IMPLANT SCANS USING TRIOS 4

Dissertação apresentada à Universidade Católica Portuguesa
para obtenção do grau de Mestre em Medicina Dentária

Ana Lia Almeida Mendes

Orientador: Professor Doutor Tiago Miguel Santos Marques
Co-Orientador: Professor Doutor Danilo Fernandes
Co-Orientador: Mestre Filipe Araújo

Viseu, 2025

Membros do Júri das Provas Públicas

Presidente: Maria José Serol de Brito Correia
Professor Associado, FMD-UCP

Arguente: André Ricardo Maia Correia
Professor Associado, FMD-UCP

Orientador: Tiago Miguel Snatos Marques
Professor Auxiliar, FMD-UCP

Data das provas públicas: 09/07/2025

"In the middle of difficulty lies opportunity"
(*Albert Einstein)*

Acknowledgments

I would like to express my deepest gratitude to my advisor, for their invaluable guidance, support, and patience throughout this journey. Your insight and encouragement have been fundamental to the development of this work.

My sincere thanks also go to my co-advisors, whose expertise, thoughtful feedback, and constant support have greatly enriched this project.

To my family, thank you for your unconditional love, strength, and belief in me. You have been my foundation in every sense, emotionally, morally, and spiritually. Your constant encouragement, even from afar or in silence, has carried me through moments of doubt and exhaustion. I am deeply grateful for everything you have done and sacrificed so that I could get to this point.

A special thank you to my grandmother, whose warmth, wisdom, and gentle presence have been a constant source of inspiration. Your love has accompanied me every step of the way.

To the one who stood by me in silence and in storm, offering quiet strength and unwavering belief, thank you for being my anchor through it all.

To my clinical partner, thank you for your collaboration, patience, and companionship throughout the practical journey. Sharing the challenges and achievements of the clinic with you made the experience richer, more balanced, and far more rewarding.

To my friends, thank you for the moments of distraction, encouragement, and motivation. Your presence made the hard times lighter and the good times even better.

This achievement would not have been possible without each of you.

ABSTRACT

Background: Intraoral scanners (IOS) are widely used in implant dentistry for capturing digital impressions, offering advantages in accuracy, efficiency, and patient comfort. However, their performance in complete-arch digital implant scanning can be affected by scanbody (SB) design and surface properties. This study aimed to evaluate the effects of SB color and geometry on scan speed and trueness using a intraoral scanner.

Materials and methods: A master cast with four angulated implants in an edentulous mandibular model was scanned using five scanbody (SB) configurations. All SBs shared the same cylindrical base design; however, they differed in the presence and design of removable flags. Three prototypes were developed for this study with removable flags of varying shapes and sizes (referred to as “ivory”, “blue”, and “small blue”), one SB had no flag (“metallic”), and one was a commercial scanbody with integrated flags (MedentiWings®, Medentika GmbH, Straumann Group, Hügelsheim, Germany). Each configuration was scanned ten times under controlled laboratory conditions using an intraoral scanner. The resulting standard tessellation language (STL) files were compared to a reference model obtained from a desktop scanner, using three-dimensional (3D) deviation analysis in Geomagic Control X® 2022 (3D Systems Inc, Rock Hill, USA). Trueness was evaluated using the root mean square (RMS) deviation. Scanning time and deviations at specific implant positions were statistically analyzed using analysis of variance (ANOVA) and Tukey’s post hoc tests.

Results: The metallic SB achieved the shortest scan time (00:47±00:06) and the highest trueness (RMS: 0.089±0.010). The ivory SB flag showed the highest deviation (RMS: 0.171±0.005) and longest scan time (01:32±00:12). MedentiWings and blue SBs flags showed intermediate performance. A statistically significant positive correlation ($p < 0.01$) was observed between scanning time and RMS deviation, indicating that longer scanning durations tend to result in reduced trueness. Additionally, deviations were consistently higher in the posterior regions than in the anterior regions, regardless of SB type.

Conclusions: SB material, color, and geometry significantly influence scan speed and trueness in full-arch implant digital impressions. Metallic SBs offered the best performance, while bright-colored or geometrically complex designs compromised accuracy and efficiency. Selecting SBs with favorable optical and geometric properties can enhance digital workflow outcomes.

Keywords: Dental Technology, Accuracy, Computer-Aided Design.

RESUMO

Introdução: Os scanners intraorais (IOS) são amplamente utilizados em implantologia por proporcionarem maior precisão, eficiência e conforto ao paciente. Contudo, o seu desempenho em digitalizações de arcadas completas pode ser influenciado por variáveis como a cor e a geometria dos scanbodies (SB). Este estudo teve como objetivo avaliar o impacto destas características na velocidade de digitalização e na fidelidade, utilizando o scanner intraoral.

Materiais e métodos: Foi digitalizado um modelo mestre de mandíbula edêntula com quatro implantes angulados utilizando cinco configurações diferentes de scanbodies (SBs). Todos os SBs apresentavam o mesmo design cilíndrico na sua base; no entanto, diferiam quanto à presença e ao formato de flags removíveis. Três protótipos foram desenvolvidos especificamente para este estudo, com flags removíveis de diferentes formas e dimensões (denominados “ivory”, “blue” e “small blue”); um SB foi utilizado sem flag (“metallic”); e um scanbody comercial com flags integradas (MedentiWings®, Medentika, Hügelsheim, Alemanha). Cada configuração foi digitalizada dez vezes, em condições laboratoriais controladas, utilizando um scanner intraoral. Os ficheiros obtidos em formato Standard Tessellation Language (STL) foram comparados com um modelo de referência obtido através de um scanner de mesa, utilizando análise tridimensional (3D) de desvios no software Geomagic Control X® 2022 (3D Systems Inc, Rock Hill, USA). A fidelidade (“trueness”) foi avaliada com base no desvio quadrático médio (RMS). O tempo de digitalização e os desvios em posições específicas foram analisados estatisticamente através de análise de variância (ANOVA) e testes post hoc de Tukey.

Resultados: O SB metálico apresentou o menor tempo de digitalização (00:47±00:06) e o desvio mais reduzido (RMS: 0,089±0,010). O SB flag marfim revelou o pior desempenho (RMS: 0,171±0,005; tempo: 01:32±00:12). Os SBs flags azuis e MedentiWings obtiveram resultados intermédios. Observou-se uma correlação positiva estatisticamente significativa ($p < 0,01$) entre o tempo de digitalização e o desvio RMS. As regiões posteriores apresentaram desvios superiores às anteriores.

Conclusões: O material, a cor e a geometria dos SB influenciam significativamente a velocidade de digitalização e a fidelidade nas impressões digitais de arcadas completas sobre implantes. Os SB metálicos apresentaram o melhor desempenho, enquanto os designs de cor clara ou geometria complexa comprometeram a precisão e a eficiência. A seleção de SB com propriedades óticas e geométricas favoráveis pode melhorar os resultados dos fluxos de trabalho digitais.

Palavras-chave: Tecnologia Dentária, Precisão, Desenho Assistido por Computador.

INDEX

TABLES INDEX

FIGURE INDEX

LIST OF ABBREVIATION

ANOVA: analysis of variance

IOS: intraoral scanners

ISO: international organization for standardization

MDC: Master digital cast

PEEK: polyether ether ketone

SB: scanbody

SBs: scanbodies

STL: standard tessellation language

$\bar{X}$**:** mean

$\tilde{X}$**:** median

s: standard deviation

1. Introduction

1. Introduction

1.1 Overview of digital implant scanning in dentistry

The field of dentistry has witnessed significant advancements over recent decades, particularly with the integration of digital technologies that have reshaped various dental specialties, especially oral rehabilitation.(1)

The 1980s and 1990s marked a turning point in dental medicine with the introduction of digital radiography and early CAD/CAM (Computer-Aided Design/Computer-Aided Manufacturing) systems.(2) These innovations revolutionized treatment planning, dramatically changing how dental prosthetics and implants were designed and manufactured.(2)

Despite the advancements brought by CAD/CAM, capturing highly accurate dental impressions has remained a challenge.(3–6) The introduction of IOS marked a significant breakthrough in digital dentistry.(3–6) These devices revolutionized impression-taking by enabling clinicians to swiftly and precisely capture 3D digital images of a patient's teeth and surrounding soft tissues.(3–6) This innovation eliminated the need for traditional physical molds, which were often uncomfortable for patients and prone to distortion or inaccuracies.(3–6) The digital impressions from IOS could be seamlessly integrated into a fully digital workflow, spanning from treatment planning to the fabrication of prosthetic components using CAD/CAM systems.(3–6) This integration streamlined the entire process, enhancing both efficiency and accuracy in dental procedures.(3–6)

The use of IOS devices has dramatically improved both the accuracy and efficiency of dental procedures.(2,6,7) Studies have shown that digital impressions produced by IOS are more accurate and reproducible than conventional methods, especially in cases of partial edentulism or single implants.(2,3,8) The digital workflow enabled by IOS not only improves patient comfort by reducing chair time but also ensures that the final prosthetic components fit more precisely, leading to better long-term outcomes for patients (2,6,7)

Accurately recording the spatial positions of implants is particularly important for achieving a passive fit in implant-supported fixed dental prostheses.(3,4,8) When digital impressions lack accuracy, the resulting restorations may require additional adjustments, potentially creating tension at the connection points between the bone and the implant, as well as between the implant and the prosthetic structure.(3,4,8,9) This tension has the potential to trigger mechanical failures in the prosthesis or biological complications in the adjacent tissues.(3,4,8,9)

1.2 Trueness and precision in digital implant scanning

Ensuring the accuracy of intraoral scanners is essential for attaining excellent clinical results, especially in implant dentistry. According to the International Organization for Standardization (ISO) 5725 standard, accuracy comprises two distinct but complementary factors: trueness and precision. Trueness measures how closely a scan matches the actual geometry of the scanned object. Precision, on the other hand, refers to the consistency of measurements, indicating how reliably similar results can be obtained in repeated scans under the same conditions.(1,3,5,7,9–16) High trueness ensures that digital impressions closely reflect the real-world geometry of teeth and implants, while high precision guarantees consistent results across multiple scans. Together, these factors determine the overall accuracy and reliability of IOS in clinical practice.(1,3,5,7,9–16)

Figure 1 Visual representation of the concepts of accuracy, trueness, and precision.

In dental implantology, achieving both trueness and precision is vital for the long-term success of implant-supported restorations.(2,4,10,17) High accuracy ensures a passive fit between the prosthetic structure and the supporting implants, minimizing the risk of mechanical complications such as screw loosening, implant fracture, or

prosthesis failure.(2,4,10,17) Studies have confirmed that digital impressions offer greater control over the accuracy of these restorations, reducing the potential for errors that can arise from manual impression techniques.(2,4,10,17) This is particularly important in cases where multiple implants are involved or when dealing with complex full-arch restorations.(2,4,10,17) Although conventional impressions may offer higher accuracy in specific full-arch cases, the differences are often clinically negligible, and digital methods continue to gain widespread adoption due to their numerous advantages.(18)

1.3 Comparison of digital methods with traditional methods

Digital scanning has emerged as a superior or similar method in implant dentistry, providing numerous advantages over conventional impression techniques. (4,19) One of the major benefits of digital workflows is the reduction in errors that can arise from the distortion of impression materials.(9,12)

Traditional methods are prone to inaccuracies due to shrinkage, expansion, or distortion of impression materials during storage and transportation, which can affect the final restoration's fit.(1,8,12)

Moreover, digital impressions have transformed dental practices by simplifying production processes and streamlining workflows.(3,7,8,16) Traditional impressions require multiple steps, including the creation of physical models from impressions and the subsequent transportation to laboratories, which introduces the possibility of errors at each stage.(3,7,8,16) Digital impressions, on the other hand, bypass these intermediary steps, allowing for the immediate electronic transmission of data to laboratories, improving efficiency and accuracy.(3,7,8,16) By storing these digital files in electronic databases, practices can enhance communication between the dentist, laboratory, and patient while eliminating the need for physical storage space.(3,7,8,16)

Another important advantage of digital scanning is the improved patient comfort.(3,10) Conventional impressions can be uncomfortable for patients, especially those with gag reflexes or limited mouth-opening.(3,9,16) The bulky trays and impression materials used in traditional methods are often challenging for these patients, whereas intraoral

scanning eliminates the need for such materials.(3,9,16) Patients experience less discomfort and the process is faster, reducing chair time and increasing overall satisfaction.(3,9,16) Digital methods also simplify the clinician's workflow by reducing operator sensitivity and allowing for easier corrections during the impression-taking process.(3,9,16)

Intraoral scanning also offers the ability to capture soft tissue details without compression, a feature that is crucial for accurately replicating the oral environment for restorations.(1) This reduces the risk of errors caused by impression material shrinkage or deformation and ensures that the digital scan more closely reflects the actual intraoral condition.(1) Digital scans are particularly advantageous in cases where soft tissue needs to be recorded precisely, as they can capture fine details that may be lost with conventional impressions.(1)

However, while digital impressions offer many benefits, some studies suggest that conventional impressions may still have an edge in terms of accuracy in certain cases, such as implant-supported restorations in fully edentulous arches.(7,16,20,21) Some studies indicate that conventional methods, particularly with splinted open-tray impression copings, may produce more accurate results in some complex implant cases.(7–9) Despite these findings, the advantages of digital scanning, particularly in terms of patient comfort, workflow efficiency, and communication, have led to its widespread adoption in clinical practice.(7–9)

1.4 Challenges in complete arch digital implant scanning

Several important factors can influence the accuracy and speed of a complete arch digital implant scan, making it essential to consider the technological, environmental, and procedural aspects involved. One of the primary factors is the type of intraoral scanner being used.(1,5,10,19) Different IOS models vary significantly in terms of the depth of field, resolution, and image capture speed they offer.(1) Some scanners are optimized for precision in capturing narrow fields, while others excel in capturing broad, detailed structures like full arches.(13) For instance, scanners such as TRIOS 4 and Primescan have been noted for their ability to capture highly accurate digital impressions even in more challenging environments like full-arch scans.(5)

The absence of anatomical reference points in edentulous arches creates a significant challenge when it comes to complete arch digital implant scanning. IOS rely heavily on stable, visible landmarks such as teeth or other hard tissue structures to accurately "stitch" together the images they capture.(3,8) In cases of edentulous patients, where there are no remaining teeth to serve as landmarks, the process of aligning and combining scanned images becomes much more complex.(3,9,17) Without these reference points, the digital scanner struggles to capture the full geometry of the arch accurately, often leading to distortions or missing data in the resulting digital impression.(3,9,17) This lack of anatomical variability can also confuse the scanner's software, resulting in poor data alignment and significant scanning errors.(3,9,17)

Another key factor is operator experience and skill.(1,5,10,19) A trained and experienced operator is more adept at optimizing the scanning process, ensuring that the scanner captures images from optimal angles while minimizing movement and avoiding common pitfalls like overexposure or poor alignment.(1,5,10,19) Experienced operators are also better at handling more complex cases, such as those involving multiple implants or full-arch scans, where meticulous attention to detail is essential.(1,5,10,19)

Finally, environmental conditions such as lighting, reflectivity, and surface properties of the scanned tissues can also affect the scanning process.(8–10) Bright lights or reflective surfaces can create unwanted glare, which confuses the scanner and results in poor data capture.(8–10) Similarly, certain soft tissue properties, such as shininess or translucency, can lead to incomplete or distorted data, affecting both accuracy and speed.(8–10)

Considering these variables, it becomes important to understand the specific characteristics of each intraoral scanner. The following table (table 1) summarizes key technical features of several commonly used IOS models, highlighting differences in scanning technology, acquisition modality, color capture, and file export formats.

Table 1 Technical characteristics of commonly used intraoral scanners.

IOS	Manufacturer	Acquisition modality	Scanner technology	Color	Export format
True definition scanner (tds)	3M ESPE	Video sequence	Active wavefront sampling	No	.STL
Trios 4	3Shape	Video sequence	Confocal microscopy	Yes	.STL, .DCM, .3OXZ
Cerec omnicam	Dentsply Sirona	Video sequence	Active triangulation with strip light projection	Yes	.STL, .DXD, .RST, .PLY
Carestream 3600	Carestream	Video sequence	Active speed 3D video	Yes	.STL, .PLY, .CSZ
Condorscan	Condor	Video sequence	Stereophotogrammetry	Yes	.STL, .PLY
Dental wings dwio	Dental Wings	Video sequence	Multiscan imaging with 10 cameras	No	.STL
Emerald	Planmeca	Video sequence	Laser triangulation	Yes	.STL, .PLY, .3OXZ
Primescan	Dentsply Sirona	Video sequence	High-frequency contrast analysis (confocal-like)	Yes	.STL, .PLY
Itero element 5d	Align Technology	Video sequence	Parallel confocal imaging	Yes	.STL, .PLY

1.5 Techniques to improve scanning accuracy

1.5.1 Use of artificial landmarks

The use of artificial landmarks is essential for enhancing the accuracy of digital scanning, particularly when natural anatomical landmarks are absent, such as in edentulous arches.(3,4,19) In these cases, intraoral scanners face challenges in accurately stitching together the digital impressions, which can result in distortions or incomplete scans.(3,4,19)

To solve this issue, artificial landmarks, such as fiducial markers or auxiliary geometric devices, are added to the scanning environment.(3,19) These markers are usually placed on the mucosa or soft tissue, providing clear, easily detectable reference points for the IOS.(3,4,22) By introducing these landmarks, the scanner gains additional data points during the triangulation process, which helps to improve the scan's accuracy by enhancing the alignment and stitching of the captured images.(3,4,22)

Beyond improving accuracy, using artificial landmarks also makes the process more efficient. The scanner can capture data more quickly, reducing the need for rescans or adjustments during the impression-taking procedure.(1,19) This leads to a smoother workflow, fewer interruptions and a higher chance of obtaining an accurate impression on the first attempt.(1,19) Research has indicated that adding artificial landmarks had a negligible impact on accuracy parameters when scanning partially edentulous cases, whereas it significantly improved the accuracy of scans for completely edentulous arches.(1,19)

1.5.2 Splinting of scanbodies

The technique of splinting SBs plays a vital role in enhancing the accuracy of digital impressions, especially for cases with multiple implants or full-arch restorations.(8,16,20) When multiple implants are involved, it's essential to preserve their precise positions relative to one another to ensure the final prosthesis fits and functions correctly.(8,16,20) However, even slight movements of the SBs during the scanning process can cause significant errors in the final impression, resulting in prosthetic misfits and the need for adjustments during manufacturing.(8,16,20)

Splinting involves connecting the SBs together with a rigid material, like biocompatible resin or metal bars, to stabilize them during the scan.(3,12,13) The splinting technique is especially effective in full-arch implant cases, where the accurate capture of multiple implant positions is critical.(3,12,13) Research has shown that splinting improves both trueness (how closely the digital impression matches the actual geometry of the arch) and precision (the scanner’s ability to consistently reproduce the same results across multiple scans).(3,12,13)

Studies have reported that using splinting techniques not only reduces the need for rescans but also improves the fit and function of the final prosthesis, resulting in better patient outcomes and fewer post-insertion adjustments.(11)

However, one study has indicated that, with TRIOS 4, splinting SBs improved the trueness of complete arch digital implant scans.(8) Other research has suggested that there is no significant advantage to splinting over non-splinted scanning when implant divergence is less than 15 degrees.(1,22)

1.5.3 Photogrammetry technology

Photogrammetry marks a significant advancement in digital implant scanning technology, providing an alternative to traditional intraoral scanning techniques, particularly in complex cases involving multiple implants or full-arch restorations.(4,14,15) Unlike intraoral scanners that rely on light triangulation to capture data, photogrammetry uses multiple cameras to capture three-dimensional images of the implant positions simultaneously.(4,14,15) This multi-camera setup allows for the capture of detailed and accurate spatial relationships between the implants without relying on the stitching process typically used in intraoral scanning.(4,14,15)

The primary advantage of photogrammetry is its ability to capture implant positions with a high degree of trueness and precision.(12) In traditional intraoral scanning, the accuracy of the final digital impression often depends on how well the scanner can stitch together the individual images it captures.(14,15,23) This can be challenging, especially in cases where anatomical landmarks are sparse or when multiple implants need to be captured in a single scan.(14,15,23) Photogrammetry eliminates the need for stitching by capturing all necessary data points in a single image, significantly reducing the likelihood of errors and distortions.(14,15,23)

Photogrammetric imaging is unable to capture soft-tissue details and therefore requires the support of intraoral scanning or conventional impressions to obtain soft-tissue information.(11,14,23)

1.6 Influence of scanbody design on digital impressions

1.6.1 Impact of scanbody geometry on scanning efficiency

Traditional vertical cylindrical SBs have long been a staple in digital implantology, valued for their simple design and ease of detection by IOS.(4,9,17) However, despite their utility in single implant procedures, they tend to present significant limitations in multi-implant and full-arch cases.(4,9,17) The main problem is their geometrically simple structure, which provides fewer reference points for the scanner to detect, thus increasing the risk of scanning inaccuracies in more complex clinical situations.(4,9,17) The simplicity of these cylindrical SBs makes it difficult for the scanner to distinguish between different positions, often leading to alignment errors.(4,9,17)

In the study of Mizumoto RM et al., a shorter, simpler SB showed the least distance deviation, making it the most accurate in terms of both trueness and precision. In contrast, taller and more complex SBs had the highest deviation.(22) A SB positioned closer to the tissue was beneficial for complete-arch scanning.(22) Additionally, the simpler SB design required the least amount of time to complete scans, while more complex designs took longer.(22)

In response to these limitations, newer SB designs have emerged that incorporate geometrically enhanced features, such as angled surfaces and lateral extensions, which offer more distinct landmarks for the scanner to detect.(9,24) These advanced designs provide the scanner with more detailed data, leading to significant improvements in both trueness and precision.(9,24) This study highlights the superiority of plasma-coated titanium SBs over traditional polyether ether ketone (PEEK) SBs, demonstrating that the complex geometry of newer designs significantly improves scanning accuracy, particularly in full-arch digital implant impressions.(9,24)

1.6.2 Effect of surface properties on scan quality

The color of SBs is a critical factor influencing the quality of intraoral scanning.(16,22) Reflective or shiny surfaces, often found in traditional metallic SBs, can cause glare, distorting the scanner's ability to capture accurate data.(16,22) This is particularly

problematic in multi-implant procedures, where the scanner needs to detect distinct reference points with high precision.(16,22)

Matte or darker-colored SBs reduce light scatter, ensuring that the scanner can capture cleaner and more accurate data.(24) This study highlights the advantages of plasma-coated titanium SBs, which, by minimizing light reflection, outperform traditional materials like PEEK in terms of both trueness and precision.(24) These non-reflective surfaces ensure that the scanner captures the implant site accurately without interference from glare.(24)

The surface properties of SBs, particularly their reflectivity and opacity, significantly affect the quality of digital impressions.(9,16,22) Highly reflective surfaces, such as polished metals, can cause light to scatter, leading to gaps and distortions in the scan data.(9,16,22) These reflective surfaces make it difficult for the scanner to capture the necessary details accurately.(9,16,22)

Furthermore, matte or opaque SBs improve workflow efficiency by reducing the need for rescans, allowing clinicians to capture accurate data in the first attempt.(9,16,22,24) This not only saves time but also improves patient satisfaction by reducing chair time.(9,16,22,24) The minimization of glare ensures that intraoral scanners can capture all necessary details accurately, resulting in better-fitting prosthetics with fewer adjustments.(9,16,22,24)

1.7 Comparison between digital scanners

IOSs offer a non-invasive, precise method for capturing three-dimensional images of dental structures. Among the most prominent systems available are Primescan® (Dentsply Sirona, York, PN, USA) and TRIOS 4® (3Shape, Copenhagen, Denmark), which employ advanced imaging technologies designed for high-resolution scanning.(25)

Primescan utilizes high-resolution sensors and shortwave light, combined Optical High-Frequency Contrast Analysis for Dynamic Deep Scanning, providing a depth capacity of up to 20 mm. It outputs data in a proprietary format (.dxd), which can be exported to an open format (.stl) via Cerec Connect®.(25) In contrast, TRIOS 4 uses

confocal microscopy and ultrafast optical scanning, generating high-quality images with output in .dcm format, which can also be exported as .stl files via Trios on Dental Desktop® system.(25)

Although both scanners are well-established, their performance varies depending on the scanning technique, materials, and clinical context.(8,24–26) Azevedo et al. demonstrated that Primescan achieved significantly higher trueness than TRIOS 4 across all techniques, including conventional, splinting, and artificial landmark scanning.(8) For TRIOS 4, the splinting technique yielded significantly higher trueness compared to the artificial landmark technique.(8)

The performance of IOSs also depends on the materials used during the scanning process.(24) Another study by Azevedo et al. reported statistically significant differences in trueness and precision across scanners with different abutment materials, except for Primescan, which remained unaffected.(24)

Plasma-coated medical titanium ISBs significantly improved trueness and precision with TRIOS 4, a result attributed to its confocal imaging technology, which interacts effectively with these ISBs.(24) Conversely, PEEK ISBs exhibited considerable variability, with Primescan achieving the highest trueness and precision, while TRIOS 4 performed the lowest.(24)

Primescan's consistent accuracy across diverse ISB materials highlights its technological superiority.(24) Unlike other systems, Primescan showed no significant differences in performance across various ISB materials, demonstrating its robustness and adaptability in diverse clinical scenarios.(24) Understanding the interaction between scanner technology and materials is essential for optimizing digital workflows in clinical dentistry.(24)

Digital scanning systems, including IOSs and laboratory scanners, exhibit distinct performance capabilities influenced by scanning distance and clinical applications.(25) Laboratory scanners consistently demonstrate superior trueness and precision, particularly over long distances, establishing them as the gold standard for accuracy.(25) Among IOSs, only iTero (Align Technologies Inc., Milpitas, CA, USA)

achieved trueness comparable to laboratory scanners for both short and long distances.(25) For shorter distances, Primescan and TRIOS 4 displayed trueness levels similar to laboratory scanners; however, precision varied, with only Primescan matching laboratory scanners in precision.(25)

In a study involving a resected maxilla from a fresh cadaver, notable differences in trueness were observed among scanners at the implant platform, depending on the operator's level of experience.(26) While increased experience with IOSs enhanced the accuracy of complete-arch superimposition, particularly in capturing palatal mucosa, but had minimal impact on implant platform trueness when soft tissues were excluded.(26) Among the evaluated systems, Primescan and TRIOS 4 achieved the highest implant platform trueness, with statistically equivalent performance.(26) These findings emphasize the advanced capabilities of Primescan and TRIOS 4 in implant platform scanning, making them preferred choices for high-accuracy requirements in implant dentistry.(26)

These results underscore the importance of selecting the appropriate scanner based on clinical objectives and highlight the need for skill development in using IOSs to optimize outcomes in complex dental procedures.

2. Objectives

2. Objectives

This study aims to evaluate the influence of SB color and geometry on the scanning speed and trueness of complete-arch digital implant impressions using a intraoral scanner. By analysing five different SB configurations, metallic, ivory, blue, small blue and MedentiWings, this research seeks to determine how variations in material and design affect the accuracy and efficiency of digital impressions.

The goal is to provide clinically relevant insights that may guide the selection of SBs for improving digital workflows in implant-supported full-arch rehabilitations.

Null hypothesis:

H_{01}: There are no statistically significant differences in scanning time between SBs of different colors.

H_{02}: There are no statistically significant differences in scanning time between SBs of different geometries.

H_{03}: There are no statistically significant differences in trueness (RMS deviation) between SBs of different colors.

H_{04}: There are no statistically significant differences in trueness (RMS deviation) between SBs of different geometries.

H_{05}: There is no statistically significant correlation between scanning time and trueness.

3. Materials and methods

3. Materials and methods

Four dental implants (Straumann BLX®**,** Institut Straumann AG, Basel, Switzerland) were initially placed in an edentulous patient. An intraoral scan of the mandibular arch was performed using a Trios 4 introral scanner (3Shape, Copenhagen, Denmark), and the resulting digital file was used to fabricate a 3D-printed definitive cast. This printed model included a soft tissue replica and served as the master model for the present study.

On this model, four angulated implant analogs (Straumann BLX®, Institut Straumann AG, Basel, Switzerland) were inserted in the positions corresponding to the lateral incisors and first molars, at a depth of 3 mm below the model's surface. To obtain a reference digital model for trueness evaluation, the master cast was scanned using a desktop scanner (Swing HD®, DOF Inc., Seoul, South Korea) with the corresponding Straumann BLX SBs. Figure 2 illustrates the digitally prepared mandible prior to 3D printing, highlighting the positioning of the scanbodies.

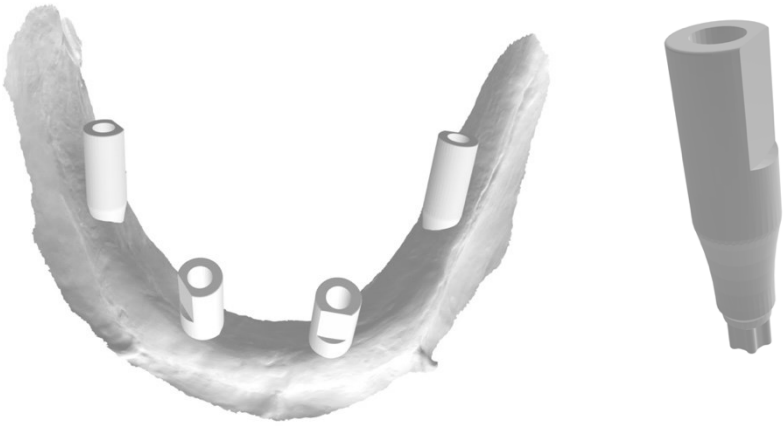

Figure 2 On the left, digital impression of an edentulous mandible prepared for 3D printing. On the right, the digital impression shows a Straumann BLX SB.

Five different SB prototypes were used for the experimental groups. Three custom-designed SBs removable flags were created using Autodesk Inventor® (Autodesk Inc., San Francisco, CA, USA) and 3D printed using a Sonic Mini 8K® printer (Phrozen

Technology Co., Ltd., Taipei, Taiwan). Among these, two prototypes were identical in shape but differed in color, one ivory and the other blue, while the third was smaller in size but the same blue color. In addition to the custom SBs, a standard metallic vertical SB and a commercially available removable flag SB, (MedentiWings®, Medentika GmbH, Straumann Group, Hügelsheim, Germany) were included in the study. Figures 3 and 4 illustrate the removable flag prototypes and the MedentiWings and metallic SBs, respectively.

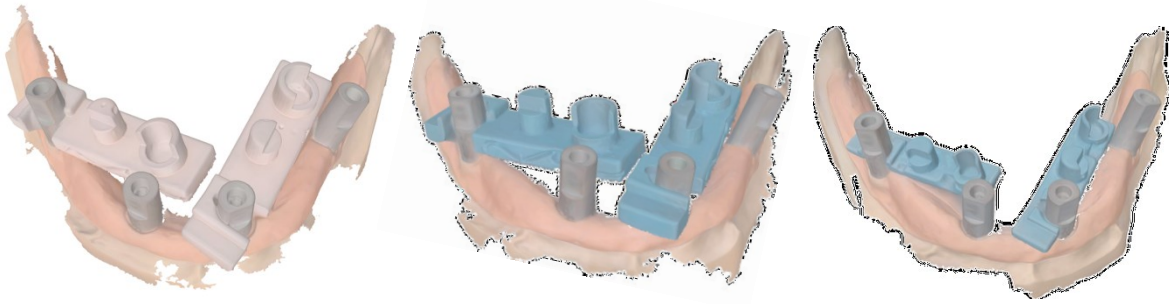

Figure 3 Prototypes of the SBs flags used in this investigation. From left to right: ivory, blue, and a smaller version in blue, respectively.

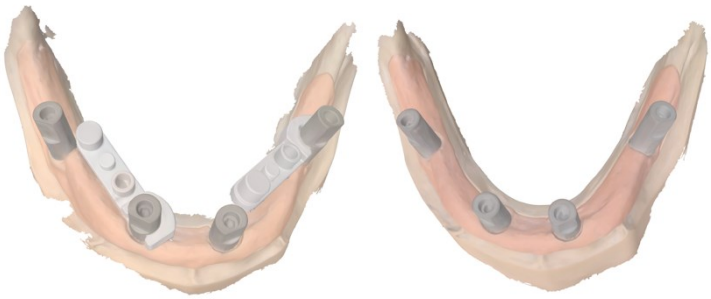

Figure 4 MedentiWings and metallic SBs.

All SBs were securely attached to the implant analogs with a torque of 5 N·cm using an automatic torque control device (Anthogyr torque wrench). They remained stationary throughout the scanning process to avoid any positional discrepancies. Each SB was visually inspected before scanning to ensure integrity and compliance with the manufacturer's specifications.

To obtain digital representations of the master model, scans were performed using the DOF Swing HD desktop scanner, which offers an accuracy of ±7 µm for implant scans according to the manufacturer. The resulting digital files were saved in STL format and designated as the master digital cast. The desktop scanner was calibrated according to the manufacturer's guidelines.

Intraoral scanning was performed using a single IOS, the Trios 4. The scanning procedure followed a zig-zag technique commonly used in previous literature, beginning with the most distal SB in the fourth quadrant.(27,28) All scans were carried out by a single experienced operator (T. M.), who had more than five years of experience with IOS technology and completed three standardized training sessions of 20 minutes each prior to the study.

Although a formal power analysis was not performed for this investigation, the sample size was determined based on previously published studies on digital complete-arch implant impressions, which followed comparable methodologies.(24,29) In those studies, statistical power analysis showed that a minimum of six scans per group was sufficient to achieve 95% power when evaluating different scanning protocols. To ensure consistency with those studies and to accommodate potential variation, a slightly larger sample size of ten scans per group was chosen. This decision is consistent with established practices in the literature and reflects the sample sizes used in similar studies assessing the trueness of intraoral scanners and scan bodies.(30–33) Consequently, ten scans were acquired for each combination of scan body type and intraoral scanner (n=10) in a temperature- and humidity-controlled environment.(34–36) The scan order was randomized using spreadsheet software (Excel; Microsoft Corp., USA). Figure 5 shows the scanned mandibular cast with SBs and soft tissue, while Figures 6 and 7 display the alignment of the SBs to the reference library and the digital representation of exported SBs with positional markers in Exocad® software (Exocad GmbH, Darmstadt, Germany), respectively.

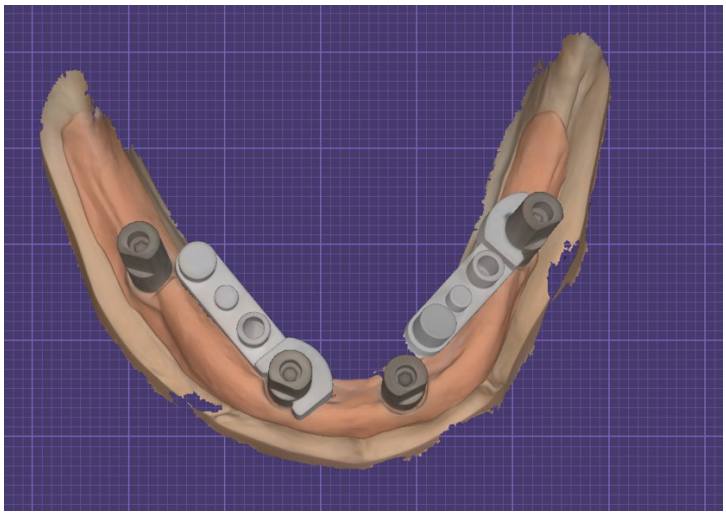

Figure 5 Visualization of the scanned mandibular cast with SBs and soft tissue using intraoral scanning software.

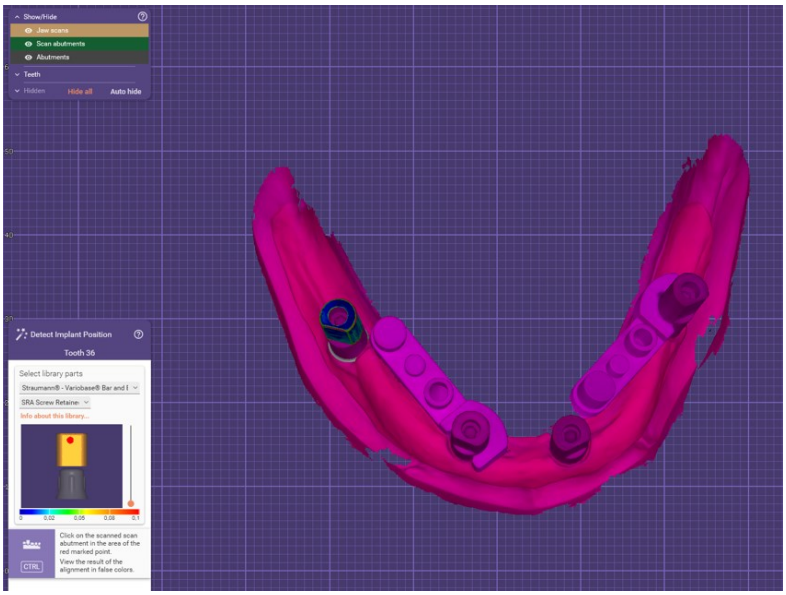

Figure 6 Alignment of SBs to the reference library using Exocad software.

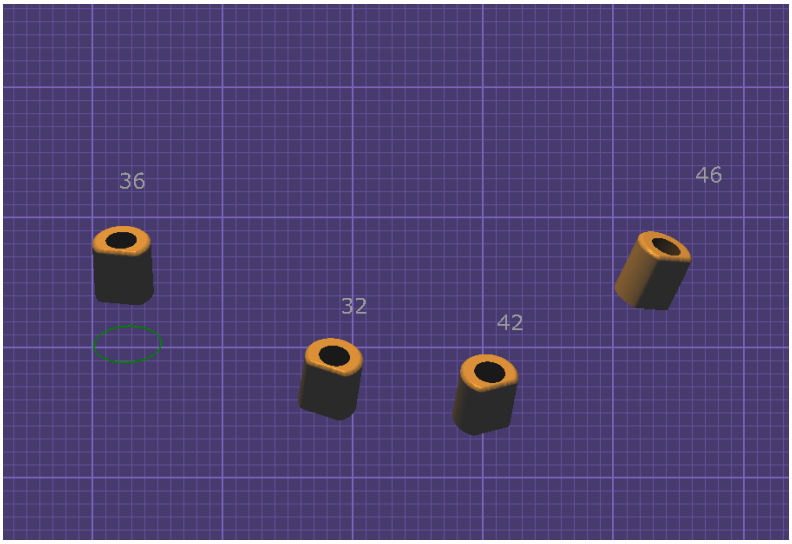

Figure 7 Digital representation of exported SBs and positional markers in Exocad software.

The STL files generated by the IOS and the desktop scanner were imported into a software program Geomagic Control X® 2022 (3D Systems Inc, Rock Hill, USA) to assess the deviation in trueness by superimposing the digital dental casts. The MDC was served as the reference.

The surfaces of the STL files were aligned for optimal superimposition by using the "Align Between Measured Data" and "Best-Fit Alignment" functions, as shown in Figure 8 and Figure 9.

The overall deviation was calculated using the "3D Compare" function, producing a color map of the superimposed digital casts to quantitatively analyse the 3D changes. The color map display deviations from +1,0 mm to −1.0mm, with a tolerance range of ±0.02mm (Figure 8). The RMS values are a statistical measure commonly used to quantify the average deviation between two datasets, particularly in the context of 3D surface analysis. In this study, the RMS was used to evaluate the differences between two superimposed digital models. The RMS serves as an indicator of the deviation value (trueness). The RMS is a mathematical parameter that measures the size of a dataset. The RMS values are calculated by first squaring the distance between each pair of corresponding points on the two surfaces. These squared deviations are then

averaged, and the square root of that average is taken to produce a single numerical value. This process ensures that all deviations are treated as positive values and that larger discrepancies have a proportionally greater influence on the result.

The RMS value provides a comprehensive assessment of the overall agreement between the compared surfaces. A lower RMS value indicates a smaller average deviation, reflecting greater geometric accuracy and higher trueness of the superimposition.

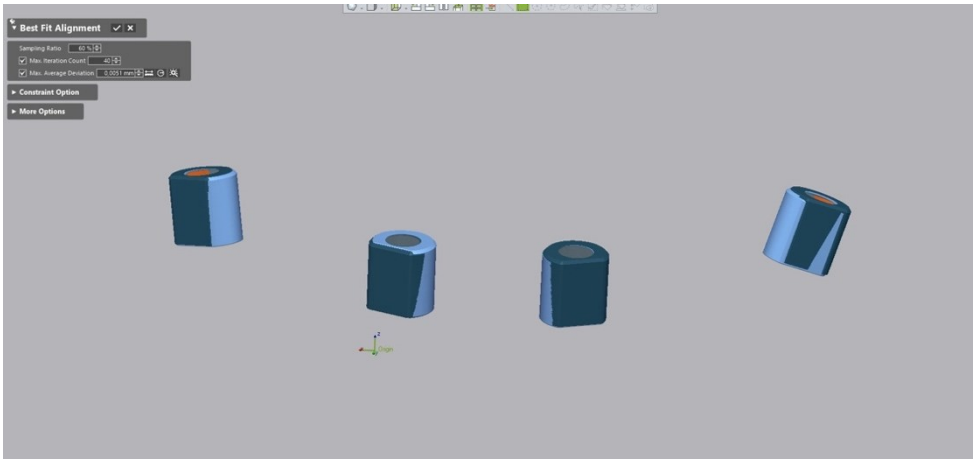

Figure 8 Best-fit alignment function in Geomagic Control X.

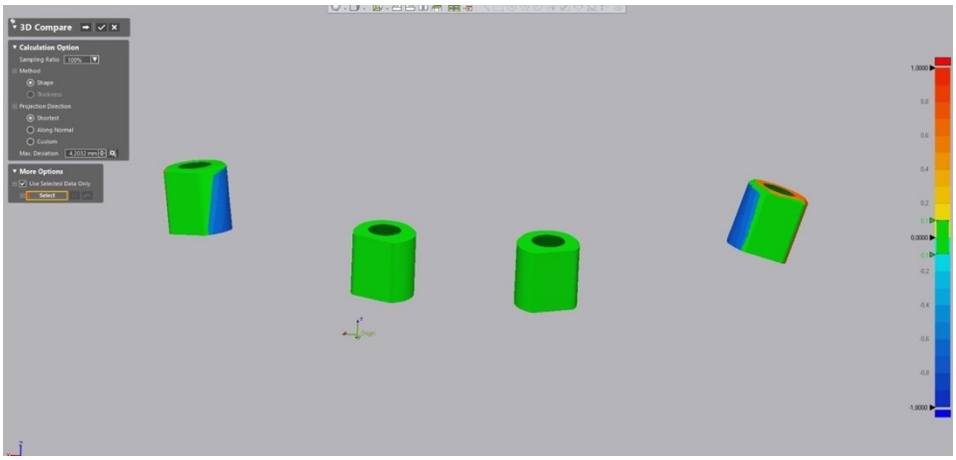

Figure 9 Color map deviation output of a scanbody showing surface variations visualized in Geomagic Control X.

The primary outcome of this study was trueness of the IOS, measured in millimeters (mm). Trueness assessed how close the digitized test object (ISBs) was to the true dimensions of the MDC.

Descriptive statistics including mean, median, standard deviation, global, minimum, and maximum values, were calculated. Initially, a random intercept mixed model was fit to account for the correlated nature of the data. Therefore, the simpler linear model was chosen. The linear model used RMS as the dependent variable, with SB type, scanning time and their interactions serving as the independent variables.

To assess the suitability of the data for parametric testing, normality tests were conducted using both the Kolmogorov-Smirnov and Shapiro-Wilk tests. These assessments were applied to the dependent variables (global RMS, position-specific RMS, minimum and maximum deviations) within each SB group. In most cases, particularly for the metallic and MedentiWings SBs flags, the data followed a normal distribution ($p > 0.05$), thereby supporting the use of parametric tests such as analysis of variance (ANOVA) and Tukey's post hoc analysis. However, in some instances, such as with the small blue and MedentiWings SBs flags at specific positions, non-normal distributions were detected ($p < 0.05$), which was considered when interpreting the results. Nevertheless, given the balanced group sizes ($n = 10$) and the robustness of ANOVA to mild deviations from normality in relatively small and homogeneous samples, parametric analysis was maintained.

ANOVA was performed to evaluate main effects and interactions, and post hoc comparisons were conducted using Tukey’s test. Precision was defined as the variability within repeated scans of the same group, while trueness was defined as the mean 3D deviation between the experimental SBs and the MDC. A significance level of $p < 0.001$ was established for all statistical tests. All analyses were carried out using SPSS Statistics® version 29.0 (IBM Corp., Armonk, New York, USA).

4. Results

4. Results

4.1 Global RMS

In this study, comparisons were performed to evaluate the influence of different removable SB flags on scanning time and the accuracy of digital impressions. The analysis focused on assessing the scanning time required for each SB, as well as the trueness of the digital models, measured by the RMS, minimum and maximum deviations in relation to the master model.

Table 2 shows the global RMS, minimum and maximum values, along with the scanning time recorded for each SB type. To determine whether there were statistically significant differences between the groups, an ANOVA test was applied to compare the results between independent groups, followed by Tukey's multiple comparison test to identify between which specific groups the differences were statistically significant

Table 2 Time characterization, global RMS, minimum and maximum relative to SB type.

SB	Time		Global average RMS		Global minimum deviation		Global maximum deviation	
	$\bar{X}$±s	$\tilde{X}$	$\bar{X}$±s	$\tilde{X}$	$\bar{X}$±s	$\tilde{X}$	$\bar{X}$±s	$\tilde{X}$
Metallic	00:47±00:06	00:47	0,089±0,010	0,090	-0,173±0,023	-0,168	0,210±0,032	0,204
Ivory	01:32±00:12	01:29	0,171±0,005	0,170	-0,390±0,013	-0,168	0,474±0,016	0,478
Blue	01:01±00:08	00:59	0,154±0,007	0,156	-0,354±0,013	-0,357	0,490±0,018	0,491
Small Blue	00:50±00:04	00:50	0,151±0,010	0,149	-0,348±0,023	-0,339	0,354±0,250	0,419
Medentika	00:54±00:11	00:56	0,121±0,006	0,121	-0,269±0,012	-0,274	0,429±0,040	0,434
T. Anova	39,168; p<0,001		180,79; p<0,001		207,78; p<0,001		9,92; p<0,001	
Tukey's multiple comparisons	Significant differences between ivory and the other groups; metallic and blue		Significant differences between all groups, except between blue and smaller blue		Significant differences between all groups, except between blue and smaller blue		Significant differences between metallic and ivory, blue, and medentika	

$\bar{X}$±s – mean ± standard deviation; $\tilde{X}$ – median

Based on the analysis of Table 1, regarding the scanning time, the lowest mean (00:47±00:06) and median (00:47) values were obtained with the metallic SB, while the highest mean (01:32±00:12) and median (01:29) values were recorded for the ivory SB. The application of the ANOVA test indicated that at least one SB group presented significantly different scanning times compared to the others. Tukey's multiple comparison test confirmed that these differences were statistically significant between the ivory SB flag and all other SB groups, as well as between the metallic SB and the blue SB flag.

Regarding the global mean RMS, the metallic SB presented the lowest deviation (0.089±0.010), whereas the ivory SB flag showed the highest (0.171±0.005). The blue

and small blue SBs flgs showed similar results, and the Medentika SB flag presented the second lowest value (0.121±0.006).

Regarding the minimum global deviation, the most extreme deviation was observed for the ivory SB flag (-0.390±0.013), whereas the highest minimum value was recorded for the metallic SB (-0.173±0.023). On the other hand, for the maximum global deviation, the highest value was obtained with the blue SB (0.490±0.018), followed by the ivory SB flag (0.474±0.016), and the lowest value was recorded for the metallic SB (0.210±0.032).

The ANOVA test indicated that at least one SB group presented statistically significant differences for the global RMS mean, minimum, and maximum values. Tukey's multiple comparison test revealed that for the global RMS mean and minimum values, statistically significant differences were observed between all SB groups, except between the blue and smaller blue SBs flags, which presented statistically similar results. Regarding the global maximum deviation values, statistically significant differences were found between the metallic SB and the ivory, blue, and Medentika SBs flags.

Figure 10 illustrates the boxplots distribution of the global mean RMS values according to the SB type.

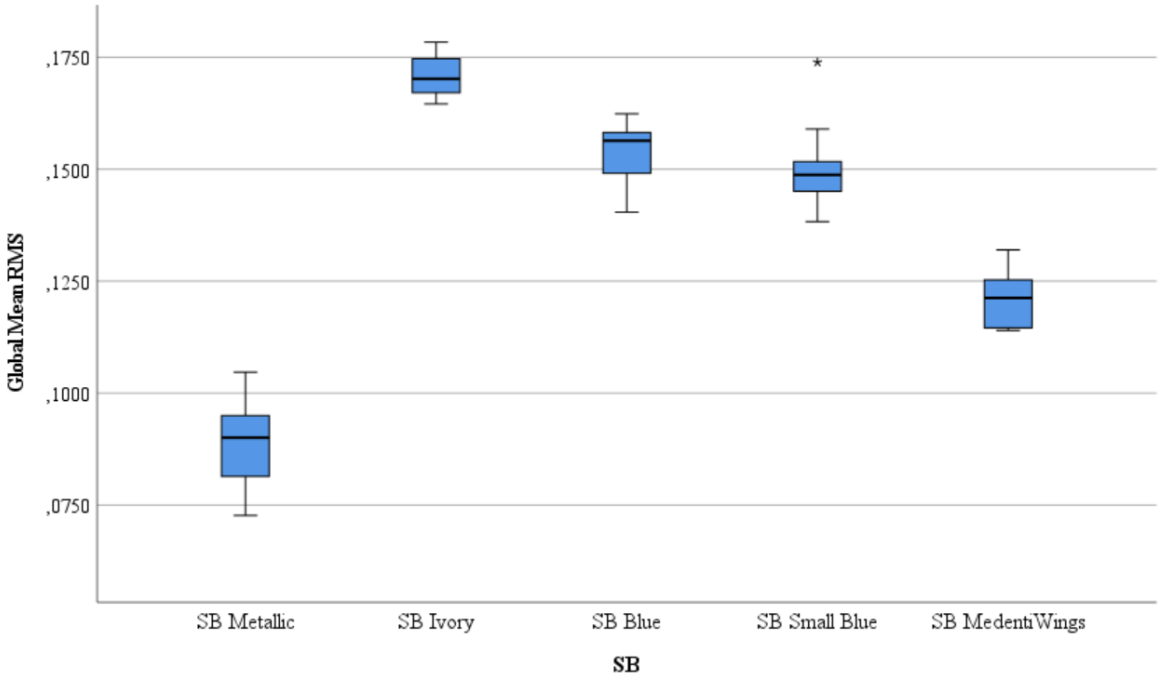

Figure 10 Boxplots of global average RMS by SB type

As illustrated in the figure 1, the distribution of the global RMS values for the metallic SB is concentrated between 0.075 and 0.100. The other distributions are located above this range, with the Medentika SB flag distribution being the next lowest, situated above the metallic SB, but lower than the remaining SB groups. In contrast, the ivory SB flag exhibited the highest RMS values and showed a very narrow distribution.

4.2 RMS analysis by SB position

4.2.1 Anterior Region

Table 3 presents the RMS results for the anterior region, specifically at positions 32 and 42 (mandibular lateral incisors, FDI notation), according to the SB type. The results are shown in terms of mean RMS, minimum and maximum deviation values for each SB group.

Table 3 Characterization of positions 32 and 42 relative to SB type.

SB		Mean RMS on position 32	Minimum deviation on position 32	Maximum deviation on position 32	Mean RMS on position 42	Minimum deviation on position 42	Maximum deviation on position 42
Metallic	$\bar{X}$±s	0,049±0,010	-0,070±0,023	0,111±0,022	0,089±0,010	-0,173±0,023	0,210±0,032
	$\tilde{X}$	0,047	-0,069	0,106	0,090	-0,168	0,204
Ivory	$\bar{X}$±s	0,133±0,003	-0,158±0,008	0,333±0,007	0,171±0,005	-0,394±0,011	0,474±0,016
	$\tilde{X}$	0,133	-0,157	0,332	0,170	-0,396	0,478
Blue	$\bar{X}$±s	0,098±0,008	-0,216±0,016	0,196±0,015	0,154±0,007	-0,354±0,013	0,490±0,018
	$\tilde{X}$	0,099	-0,216	0,197	0,156	-0,357	0,491
Small Blue	$\bar{X}$±s	0,097±0,005	-0,208±0,010	0,184±0,009	0,151±0,010	-0,348±0,028	0,425±0,045
	$\tilde{X}$	0,099	-0,203	0,186	0,149	-0,339	0,419
Medentika	$\bar{X}$±s	0,096±0,023	-0,249±0,069	0,227±0,062	0,121±0,006	-0,269±0,012	0,429±0,040
	$\tilde{X}$	0,103	-0,269	0,242	0,121	-0,274	0,434
T. Anova		61,75; p<0,001	42,41; p<0,001	70,41; p<0,001	180,79; p<0,001	219,99; p<0,001	121,43; p<0,001
Tukey's multiple comparisons		Significant differences between all groups, except between blue, small blue and medentika	Significant differences between all groups, except between blue, small blue and medentika	Significant differences between all groups, except between blue, small blue and medentika	Significant differences between all groups, except between blue, small blue and medentika	Significant differences between all groups, except between blue and small blue	Significant differences between all groups, except between ivory and blue, and between small blue and Medentika

$\bar{X}$±s – mean ± standard deviation; $\tilde{X}$ - median

Based on the analysis of the table 2, at position 32, the lowest mean RMS value was observed for the metallic SB (0.049±0.010), while the highest value was recorded for the ivory SB flag (0.133±0.003). Regarding the minimum deviation at this position, the most extreme value was found in the Medentika SB flag (-0.249±0.069), whereas the value closest to zero was recorded in the metallic SB (-0.070±0.023). Concerning the maximum deviation at position 32, the lowest value was observed in the metallic SB (0.111±0.022), and the highest value in the ivory SB flag (0.333±0.007).

The application of the ANOVA test indicated that at least one SB group presented significantly different results for the mean RMS, minimum, and maximum deviation

values at position 32. According to Tukey's multiple comparisons test, these differences were statistically significant across all groups, except between the blue, small blue, and Medentika SB flags.

At position 42, the lowest mean RMS value was recorded in the metallic SB (0.089±0.010), and the highest in the ivory SB flag (0.171±0.005). Regarding the minimum deviation value, the most extreme result was found in the ivory SB flag (-0.394±0.011), while the closest to zero was observed in the metallic SB (-0.173±0.023). For the maximum deviation value at position 42, the lowest result was found in the metallic SB (0.210±0.032), and the highest in the blue SB (0.490±0.018).

The ANOVA test confirmed that at least one SB group presented significantly different results for the mean RMS, minimum, and maximum deviation values at position 42. Tukey's multiple comparisons test revealed that these differences were statistically significant between all groups, except between the blue and small blue SBs flags for the mean RMS and minimum deviation values, and between the blue, small blue, and Medentika SBs flags for the maximum values.

4.2.2 Posterior Region

Table 4 presents the RMS results for positions 36 and 46 (mandibular first molars, FDI notation) according to the SB type. The results are shown in terms of mean, minimum, and maximum RMS values for each SB group.

Table 4 Characterization of RMS at positions 36 and 46 according to SB type.

SB		Mean RMS on position 36	Minimum deviation on position 36	Maximum deviation on position 36	Mean RMS on position 46	Minimum deviation on position 46	Maximum deviation on position 46
Metallic	$\bar{X}$±s	0,117±0,015	-0,131±0,112	0,209±0,031	0,100±0,018	-0,155±0,026	0,164±0,033
	$\tilde{X}$	0,116	-0,157	0,204	0,099	-0,151	0,161
Ivory	$\bar{X}$±s	0,160±0,008	-0,250±0,013	0,290±0,015	0,237±0,009	-0,350±0,015	0,474±0,016
	$\tilde{X}$	0,159	-0,251	0,292	0,238	-0,352	0,478
Blue	$\bar{X}$±s	0,162±0,011	-0,232±0,019	0,301±0,022	0,228±0,009	-0,354±0,013	0,490±0,018
	$\tilde{X}$	0,167	-0,236	0,310	0,231	-0,357	0,491
Small Blue	$\bar{X}$±s	0,149±0,018	-0,210±0,024	0,267±0,030	0,220±0,018	-0,348±0,028	0,370±0,198
	$\tilde{X}$	0,142	-0,201	0,254	0,217	-0,339	0,419
Medentika	$\bar{X}$±s	0,116±0,020	-0,172±0,029	0,242±0,038	0,143±0,019	-0,262±0,012	0,413±0,044
	$\tilde{X}$	0,118	-0,176	0,248	0,148	-0,259	0,419
T. Anova		22,05; p<0,001	7,87; p<0,001	17,35; p<0,001	160,82; p<0,001	188,73; p<0,001	19,94; p<0,001
Tukey's multiple comparisons		Significant differences between all groups, except among ivory, blue, and small blue; and between metallic and Medentika	Significant differences between metallic and ivory, blue, and small blue, and also between ivory and Medentika	Significant differences between metallic and ivory, blue, and small blue; between ivory and Medentika; and between blue and Medentika	Significant differences between all groups, except among ivory, blue, and small blue; and between blue and small blue	Significant differences between all groups, except among ivory, blue, and small blue; and between blue and small blue	Significant differences between metallic and the other groups

$\bar{X}$±s – mean ± standard deviation; $\tilde{X}$ - median

For position 36, the lowest mean RMS value was recorded for the Medentika SB flag (0.116±0.020), closely followed by the metallic SB (0.117±0.015), while the highest mean RMS value was observed in the blue SB flag (0.162±0.011). Regarding the minimum deviation value at this position, the most extreme value was found in the ivory SB flag (-0.250±0.013), whereas the value closest to zero was recorded in the metallic SB (-0.131±0.112). Concerning the maximum deviation value for position 36, the lowest result was observed in the metallic SB (0.209±0.031), and the highest in the blue SB flag (0.301±0.022).

The application of the ANOVA test indicated that at least one SB group presented significantly different results for the mean RMS, minimum, and maximum deviation values at position 36. According to Tukey's multiple comparisons test, the differences observed for the mean RMS between the metallic SB and Medentika SB flag were not statistically significant, as well as the differences between the ivory, blue, and small blue SBs flags. The remaining comparisons showed statistically significant differences.

For the minimum deviation, statistically significant differences were found between the metallic, ivory, blue, and small blue SBS flags; between the ivory and Medentika SBs flags; and between the blue and Medentika SBs flags.

Regarding position 46, the lowest mean RMS value was recorded for the metallic SB (0.100±0.018), while the highest was observed for the ivory SB (0.237±0.009). For the minimum at this position, the most extreme result was found in the blue SB flag (-0.354±0.013), whereas the value closest to zero was recorded in the metallic SB (-0.155±0.026). Concerning the maximum value at position 46, the lowest result was observed in the metallic SB (0.164±0.033), and the highest in the ivory SB flag (0.474±0.016).

The ANOVA test showed that at least one SB group presented statistically significant differences for the mean RMS, minimum, and maximum deviation values at position 46. According to Tukey's multiple comparisons test, for the mean RMS and minimum values, statistically significant differences were found between all groups, except between the ivory, blue, and small blue SBs flags, and between the blue and small blue SBs flags. For the maximum values, statistically significant differences were observed between the metallic SB and all other SB flags.

4.3 Deviations analysis for anterior vs. posterior region

Table 5 presents the deviations results for the anterior (positions 32 and 42) and posterior (positions 36 and 46) regions according to the SB type.

Table 5 Characterization of RMS, minimum and maximum deviation at anterior and posterior regions according to SB type.

SB		Mean RMS posterior region	Minimum deviation posterior region	Maximum deviation posterior region	Mean RMS anterior region	Minimum deviation anterior region	Maximum deviation anterior region
Metallic	$\bar{X}$±s	0,109±0,016	-0,143±0,048	0,187±0,029	0,069±0,008	-0,121±0,016	0,160±0,017
	$\tilde{X}$	0,108	-0,155	0,181	0,070	-0,126	0,161
Ivory	$\bar{X}$±s	0,198±0,008	-0,300±0,014	0,382±0,015	0,152±0,004	-0,276±0,006	0,403±0,006
	$\tilde{X}$	0,199	-0,300	0,387	0,152	-0,276	0,404
Blue	$\bar{X}$±s	0,195±0,009	-0,293±0,016	0,396±0,019	0,126±0,006	-0,285±0,012	0,343±0,014
	$\tilde{X}$	0,200	-0,299	0,403	0,125	-0,284	0,341
Small blue	$\bar{X}$±s	0,185±0,017	-0,279±0,025	0,319±0,109	0,124±0,006	-0,278±0,018	0,304±0,024
	$\tilde{X}$	0,180	-0,268	0,338	0,123	-0,272	0,299
Medentika	$\bar{X}$±s	0,129±0,019	-0,217±0,015	0,327±0,041	0,109±0,011	-0,259±0,040	0,328±0,023
	$\tilde{X}$	0,132	-0,218	0,331	0,112	-0,272	0,333
T. Anova		80,79; p<0,001	61,95; p<0,001	22,74; p<0,001	171,01; p<0,001	102,20; p<0,001	248,21; p<0,001
Tukey's multiple comparisons		Significant differences between all groups, except among ivory, blue, and small blue;	Significant differences between all groups, except among ivory, blue, and small blue;	Significant differences between metallic and the other groups	Significant differences between all groups, except between blue and small blue	Significant differences between metallic and the other groups	Significant differences between all groups, except between Medentika and blue and small blue

$\bar{X}$±s – mean ± standard deviation; $\tilde{X}$ - median

Based on the analysis of the table 4, for the posterior region, the lowest mean RMS value was recorded for the metallic SB (0.109±0.016), while the highest was observed for the ivory SB flag (0.198±0.008). Regarding the minimum deviation for this region, the most extreme value was found in the ivory SB flag (-0.300±0.014), whereas the value closest to zero was observed in the metallic SB (-0.143±0.048). Concerning the maximum deviation value for the posterior region, the lowest value was recorded in the metallic SB (0.187±0.029), and the highest in the blue SB flag (0.396±0.019).

The application of the ANOVA test indicated that at least one SB group presented statistically significant differences for the mean RMS, minimum, and maximum

deviation values for the posterior region. According to Tukey's multiple comparisons test, for both the mean RMS and minimum deviation values, statistically significant differences were observed between all groups, except between the ivory, blue, and small blue SBs flags, and between the blue and small blue SBs flags. Regarding the maximum deviation values, statistically significant differences were found between the metallic SB and all other SBs flags.

Considering the mean RMS results for the anterior region, the lowest value was recorded for the metallic SB (0.069±0.008), and the highest for the ivory SB flag (0.152±0.004). Regarding the minimum deviation at this position, the most extreme value was observed in the blue SB flag (-0.285±0.012), while the value closest to zero was recorded in the metallic SB (-0.121±0.016). Concerning the maximum deviation value for the incisors, the lowest result was found in the metallic SB (0.160±0.017), and the highest in the ivory SB flags (0.403±0.006).

The ANOVA test showed that at least one SB group presented statistically significant differences for the mean RMS, minimum, and maximum deviation values for the anterior region. According to Tukey's multiple comparisons test, for both the mean RMS and maximum deviation values, statistically significant differences were observed between all groups, except between the blue and small blue SBs flags, and between the Medentika, blue, and small blue SBs flags for the maximum deviation. For the minimum deviation, statistically significant differences were found between the metallic SB and all other SBs flags.

4.4 Correlation between scanning time and RMS

Table 6 presents the Pearson correlation coefficients between the scanning time and the mean RMS values (global and for each position).

Table 6 Pearson Correlation Between Scanning Time and Mean RMS.

RMS global	RMS 32	RMS 42	RMS 36	RMS 46	RMS of posterior region	RMS of anterior region
0,615**	0,662**	0,615**	0,453**	0,509**	0,506**	0,668**

**-significant at 1%

Based on the previous analysis, it was concluded that the correlations between the scanning time and the mean RMS values are statistically significant at a 1% significance level and are positive. Therefore, it can be stated that there is a linear relationship between the scanning time and the deviations, as the scanning time increases, the deviations also increase. It was also concluded that the strength of this relationship is moderate, being more relevant for RMS at the anterior region.

Figure 11 presents the mean RMS results for the anterior and posterior regions according to the type of SB.

Figure 11 Mean RMS values sccording to position and SB type.

Based on the data presented in figure 10, it can be observed that the posterior region exhibited higher deviations across all SB types. For both positions analyzed, the lowest mean RMS values were recorded for the metallic SB, followed by the Medentika SB flag.

The application of a two-way ANOVA (considering position and SB type) showed that the results were statistically different between positions (posterior versus anterior) ($p<0.001$) and between SB types ($p<0.001$). Specifically, the metallic SB presented

significantly lower deviations compared to all other SBs flags, the Medentika SB flag showed significantly lower deviations than the blue SB flag, the ivory SB flag exhibited significantly higher deviations than all other SB types, and the blue SB showed results statistically similar to the small blue SB flag.

5. Discussion

5. Discussion

This study aimed to assess the effects of SB color and geometry on scanning time and trueness in complete-arch digital implant impressions using the Trios 4 intraoral scanner. To guide the analysis, five null hypotheses were established: (H_{01}) that there would be no statistically significant differences in scanning time between SBs of different colors; (H_{02}) no significant differences in scanning time between SBs of different geometries; (H_{03}) no significant differences in trueness between SBs of different colors; (H_{04}) no significant differences in trueness between SBs of different geometries; and (H_{05}) no statistically significant correlation between scanning time and trueness.

The findings of this study led to the rejection of all five null hypotheses. Statistically significant differences were observed in scanning time and trueness across SBs of varying colors and geometries. The metallic SB demonstrated the shortest scanning time and the highest trueness, while the ivory SB flag exhibited the longest scanning time and the lowest trueness. Furthermore, a statistically significant positive correlation was identified between scanning time and RMS deviation, indicating that increased scanning durations were associated with greater inaccuracies. These results confirm that both the visual properties (such as color and surface reflectivity) and geometric design of SBs have a direct impact on the performance of intraoral scanning.

5.1 Factors influencing the accuracy of intraoral scanners

The accuracy of IOS in capturing complete-arch implant impressions is a multifactorial outcome that can be influenced by a variety of operator-related, patient-related, and technical factors. As described by Azevedo et al. and Revilla-León et al., variables such as the operator's clinical experience, scanning technique, scanning distance, the scanning strategy employed, and environmental conditions, including ambient lighting, temperature, and humidity, all play a crucial role in the final trueness and precision of the digital impression.(24,37)

The characteristics of the intraoral environment, such as the presence of saliva, patient movement, limited mouth opening, and accessibility to posterior areas, can further compromise the accuracy of IOS scans, particularly in complete-arch rehabilitations.(37,38)

In order to minimize the impact of these external variables and to ensure that the results of the present study were solely attributable to the type of SB evaluated, all digital impressions in this investigation were performed by the same experienced operator. This approach aimed to reduce potential inconsistencies associated with operator variability, as differences in scanning skills, speed, or technique between operators could introduce additional biases or errors in the acquisition phase. The operator had prior extensive training and experience with the IOS device used in the study, which is recognized as a critical factor for obtaining accurate results.(24,37)

The IOS device used was calibrated according to the manufacturer's instructions before each scanning session, ensuring optimal performance and accuracy.

Moreover, all scans were performed under controlled laboratory conditions, ensuring a standardized environment throughout the data acquisition process. The ambient temperature and lighting conditions were maintained constant for all impressions, eliminating the influence of external environmental factors that have been shown to interfere with the optical systems of IOS devices.(39)

In the present study, a zig-zag scanning technique was employed for all digital impressions. This scanning path is frequently recommended in the literature for complete-arch digital implant procedures, as it facilitates continuous data acquisition and minimizes abrupt directional changes that could disrupt image stitching.(27,28)

However, it is important to recognize that the literature does not provide a clear consensus regarding the most suitable scanning pattern for complete-arch implant impressions. Different IOS devices may respond variably to certain scanning strategies depending on their acquisition technology and image stitching algorithms.(24) Some studies suggest that the zig-zag pattern may offer advantages in specific situations, particularly for edentulous arches or cases with multiple implants.(24,27,28)

Despite this, other evidence indicates that certain scanning patterns might penalize the accuracy of specific IOS devices, especially when dealing with long-span scans or when the distance between implants increases.(40) Increasing the distance between implants leads to higher deviations due to the cumulative effect of image stitching errors.(40)

Rutkūnas et al. confirmed that the highest deviations occur between SBs positioned at long distances from each other, particularly in the mandible.(38) The absence of anatomical landmarks in edentulous arches further exacerbates this issue, as highlighted by Iturrate et al. and Cheng et al.(4,41) Although the present study did not specifically analyse the impact of interimplant distance, this factor should be acknowledged as a potential limitation.

5.2 Influence of scanbody geometry and color on accuracy

The primary objective of the present study was to evaluate how the geometry and color of SBs affect the accuracy of full-arch digital implant impressions. The accuracy of digital impressions is a critical factor in the success of implant-supported prosthetic rehabilitations, as inaccuracies can lead to misfit of the final restoration and potential biological or mechanical complications.(8,16,20,42) Considering the growing integration of IOS in clinical practice, understanding the influence of SB characteristics on scan accuracy is essential to optimize clinical workflows.

The results demonstrated that the metallic SB group exhibited the lowest RMS values, indicating superior trueness compared to other SB types. These findings align with those of Meneghetti et al., who reported that SB design and material significantly affect scanning accuracy.(9) Their study showed that SBs with a cylindrical shape and reduced height provided the highest accuracy, emphasizing the importance of geometry and material properties in SB performance.(9)

The superior performance of metallic SBs observed in the present study may be attributed to their rigidity and favorable optical properties. Metallic SBs are less prone to deformation during scanning and provide a more stable reference for the IOS device.

This observation contrasts with findings by Huang et al., who reported that SBs with extensional structures improved scanning accuracy.(16)

Additionally, Azevedo et al. confirmed that plasma-coated medical titanium SBs provide greater accuracy than PEEK SBs, although both materials remain within clinically acceptable thresholds (<120 μm).(24) The present study supports this conclusion, as metallic SBs consistently outperformed other materials, particularly the ivory SB group, which exhibited the highest RMS deviations.

Regarding the Medentika scanbody flag, characterized by its matte white color and removable flag design, it demonstrated better performance than both the blue and small blue scanbody flags. Although its accuracy did not exceed that of the metallic scanbody, the results suggest that its geometry and surface characteristics may enhance scanner recognition. In particular, the lower surface reflectivity of the Medentika scanbody, compared to the more reflective ivory and blue scanbodies, may have contributed to improved light capture and reduced scanning artifacts. This more favorable optical behavior likely supports more consistent and accurate data acquisition during the scanning process.

The blue and small blue SBs flags showed similar performance, with RMS values higher than Medentika SB flag and metallic SB but lower than ivory SB flag. These SBs flags incorporate complex geometrical markers designed to aid scanning; however, their light color and potential differences in reflectivity or surface finish might have introduced limitations. Although geometrically detailed, these SBs flags did not achieve the same level of accuracy, indicating that design complexity alone may not be sufficient without appropriate material properties.

The ivory SB removable flag consistently presented the highest RMS values across all measurements, indicating the lowest trueness among the SBs tested. Despite sharing a similar removable flag geometry with the other colored SBs, its pale coloration and possible differences in surface texture likely impaired scanner recognition. These findings suggest that highly reflective or bright-colored SBs flags may be more prone to inaccuracies due to challenges in light capture and image stitching by the IOS.

Although the present study identified significant differences in scan accuracy based on SB geometry and color, these findings contrast with those reported by Lu et al. (2025), who evaluated a 3D-printed custom resin scan crossbar (3D-CRC) and achieved markedly higher accuracy. Their study demonstrated mean RMS deviations as low as 43.3 ± 19.1 µm in vivo, significantly outperforming all SB types evaluated in the current investigation. While Lu et al. attributed this improvement to the added geometric reference markers and the stabilizing effect of the crossbar structure, our results suggest that such enhancements in scanbody design alone may not guarantee superior performance, particularly when paired with suboptimal surface properties or light-reflective materials. This discrepancy highlights that material characteristics and scanner detectability remain critical limiting factors, and that different designs may perform inconsistently depending on the scanning context and conditions.(43)

5.2.1 Positional influence on trueness

The results of this study demonstrated that SB performance varied not only by design and color but also by implant position within the arch. RMS values were consistently higher at the posterior region (position 36 and 46) compared to the anterior sites (32 and 42) across all SB types. This trend suggests that the distance between implants and their placement in less accessible regions significantly contributes to scan distortion.

Posterior segments are more susceptible to cumulative image stitching errors, particularly in edentulous arches lacking anatomical landmarks. The absence of reliable topographic references in these regions may cause IOS software to misalign or interpolate inaccurately. These findings align with the work of Rutkūnas et al. and Iturrate et al., who emphasized how scan accuracy diminishes over longer spans, especially when anatomical reference points are sparse.(4,38)

Tan MY et al. further highlighted that increasing interimplant distances significantly contribute to the accumulation of stitching errors in full-arch digital impressions, supporting the trend observed in the present investigation.(40)

5.2.2 Maximum and minimum deviations among scanbodies

Beyond mean RMS values, the range of deviation, including minimum and maximum, offers insight into each SB's reliability, predictability, and risk for outliers. Notably, the ivory SB flag exhibited the greatest negative deviation (-0.390 mm), while the blue SB flag presented the highest positive deviation (0.490 mm). These extreme values highlight a potential clinical risk: even if a SB appears accurate on average, the occasional occurrence of large deviations may compromise the fit of the final prosthesis or require time-consuming adjustments.

This variability becomes especially significant in full-arch implant cases, where even minor discrepancies can propagate into significant alignment issues across the prosthetic span. If a SB cannot consistently maintain its positional integrity during scanning, it introduces uncertainty and may undermine confidence in the digital impression's fidelity.

Therefore, it is essential to assess not only the central tendency (mean trueness) but also the spread and distribution of errors. A narrow deviation range indicates better repeatability and a reduced likelihood of clinical complications due to misfit. The findings of this study showed that the metallic SB offered the most stable performance, with consistently low RMS values and minimal fluctuation across all implant positions. In contrast, the blue and ivory SBs flagsexhibited higher and more variable extremes, suggesting less predictable outcomes.

These results support the clinical recommendation to prioritize SBs that demonstrate both high accuracy and low variability. Such selection enhances the predictability of digital workflows, minimizes the risk of remakes, and contributes to more efficient and reliable patient care.

5.3 Analysis of the influence of scan aids and splinting techniques

The literature extensively discusses the use of auxiliary devices, scan aids, and splinting techniques to improve the accuracy of full-arch implant impressions. Eddin and Önöral demonstrated that the use of 3D-printed scan aids significantly reduced

distortion, achieving accuracy comparable to conventional impressions.(3) However, the present study achieved superior accuracy using metallic SBs without the need for splinting or auxiliary aids, suggesting that appropriate material selection may eliminate the necessity for additional stabilization techniques.

Similarly, Nedelcu et al. found that the standard scanning protocol produced better trueness and precision results than those using splinting or dental floss stabilization.(11) These findings align with the present study, reinforcing the idea that high-quality SB materials can independently enhance scanning accuracy without the need for complex scanning aids.

Contrastingly, Iturrate et al. emphasized the positive impact of auxiliary geometric devices on trueness and precision, particularly over longer scanning distances.(4) Nevertheless, Canullo et al. reported no significant improvement in accuracy when auxiliary geometric devices were used with certain IOS devices, including Trios 3 and Carestream 3700.(19) The present study supports Canullo's findings, as high accuracy was obtained without auxiliary geometric devices, highlighting the sufficiency of metallic SBs for achieving precise digital impressions.

Another technique is presented by Etxaniz et al., who proposed the use of a geometric pattern framework to improve the trueness of full-arch digital scans.(44) Their approach involves capturing multiple short-span scans around each SB and then superimposing them with the aid of a geometric reference structure using CAD software. This technique aims to reduce stitching errors that are typically associated with longer spans in edentulous arches.(44) Their findings showed improved scan accuracy compared to conventional long-span scanning.(44)

In contrast to the above-mentioned techniques, the present study demonstrated that superior accuracy was achieved using a standard metallic SB when compared to SBs incorporating removable flags with geometric features. While these removable flag SBs were designed to enhance scanner detection through complex geometry, their performance was consistently inferior to that of the metallic SB across all evaluated parameters. This finding suggests that material properties such as rigidity and surface

reflectivity had a more substantial impact on scan accuracy than added structural complexity.

Therefore, although auxiliary aids and geometric patterns, as described by Etxaniz et al. and others, can improve scan trueness, this study confirms that a well-designed, high-performance metallic SB can achieve comparable or superior accuracy without additional supports, offering a more streamlined and clinically practical approach.

5.4 Clinical implications

The outcomes of this investigation bear significant weight for everyday clinical practice, particularly for prosthetically driven implant procedures involving digital workflows. First and foremost, the study reaffirms that the design and material characteristics of SBs, specifically their geometry, surface texture, and reflectivity, play a pivotal role in influencing both the efficiency and accuracy of intraoral scans.

Clinicians are therefore encouraged to prioritize SBs that exhibit simplified geometries and matte surface finishes, such as plasma-coated metallic variants. These designs not only facilitate quicker data acquisition but also ensure a higher degree of trueness, thereby reducing the likelihood of prosthetic misfit or the need for time-consuming chairside adjustments.

On the other hand, the use of aesthetically tailored or brightly colored SBs, while visually distinctive, may compromise scan integrity. Reflective or light-colored surfaces can interfere with optical data acquisition, leading to distorted digital impressions. In the long term, such inaccuracies may manifest as occlusal imbalances or even implant complications, all of which can erode patient trust and increase clinical workload.

The clinical implications are clear: a thoughtful approach to SB selection, grounded in evidence rather than appearance or convenience, can profoundly influence the predictability and long-term success of implant rehabilitations. Reducing scanning time and enhancing trueness ultimately translates into better prosthetic fits, improved patient outcomes, and a more efficient clinical workflow.

5.5 Strengths and limitations

This study presents several notable strengths that reinforce the validity of its findings. The controlled experimental design stands out as a key strength of this study, as it minimized the impact of extraneous variables. All scans were conducted under standardized laboratory conditions by a single experienced operator using a calibrated Trios 4 IOS. This consistency in methodology ensured that the observed differences in scanning outcomes could be confidently attributed to variations in SB design and color, rather than operator technique or environmental inconsistency.

Furthermore, the use of a high-precision desktop scanner to generate a reference master model provided a robust baseline against which trueness could be objectively assessed. The adoption of well-established analytical tools, such as 3D superimposition and RMS deviation calculations, further strengthened the scientific rigor of the study.

Nevertheless, some limitations warrant discussion. Firstly, the in vitro nature of the study does not fully replicate clinical conditions. In real-world scenarios, patient-related variables such as involuntary movement, tongue interference, saliva, and restricted intraoral access can negatively affect scan quality. These dynamic factors may introduce deviations not observed in a laboratory setting. The main limitations of this study include its in vitro design and the use of a single operator, which may limit the generalizability of the results to real-world clinical settings. Future research should address these limitations by evaluating the influence of SB characteristics in vivo, with multiple operators and under more complex anatomical conditions.

Secondly, only one intraoral scanner model (Trios 4) was evaluated. While it is widely validated and clinically adopted, results may vary with other IOS systems, especially those using different imaging technologies (e.g., structured light vs. confocal microscopy) or processing algorithms. Broader comparisons would enhance the generalizability of these findings.

Thirdly, number and type of SBs assessed were limited to five distinct designs. Although representative, they do not encompass the full range of commercially available or custom-fabricated SBs. A more extensive evaluation, including various materials (e.g., PEEK, zirconia), surface coatings (e.g., matte, plasma-sprayed), and geometric configurations (e.g., splinted, crossbar-supported), would provide more comprehensive clinical guidance.

Lastly, precision was not statistically analyzed in depth in this study. While trueness was emphasized, future studies may benefit from a dual approach that includes repeatability across multiple sessions and operators to fully capture IOS performance variability.

5.6 Future research directions

Building on the insights gained from this study, several promising avenues for future research can be proposed. One essential direction is the evaluation of SB performance in vivo. Clinical studies are needed to confirm whether the superior performance of metallic and geometrically simpler SBs under controlled conditions holds true in complex, real-life environments. Variables such as patient movement, saliva, mucosal dynamics, and limited visibility may significantly affect scanning fidelity.

Additionally, expanding the range of SB materials, geometries, and surface finishes tested across a variety of IOS platforms would help establish standardized guidelines for device compatibility and scan optimization. Comparative studies involving emerging scanner technologies, such as those employing photogrammetry or artificial intelligence-based image reconstruction, may reveal opportunities to further reduce scan times while enhancing trueness.

Future investigations could also explore the development and validation of adaptive scanning protocols that respond dynamically to scan complexity and patient anatomy. For instance, real-time software feedback mechanisms could guide the clinician on optimal scanning angles, detect potential stitching errors early, or recommend rescan regions proactively.

Lastly, interdisciplinary collaboration between dental researchers, software engineers, and materials scientists may facilitate the innovation of next-generation scanbodies that harmonize ideal geometry, low reflectivity, and ease of use. These innovations could pave the way toward a more predictable, patient-centered, and efficient digital implant workflow.

6. Conclusion

6. Conclusion

This study demonstrates that SB material, color, and geometry have a significant impact on both the scanning speed and trueness of full-arch digital implant impressions using the Trios 4 intraoral scanner. Metallic SBs consistently delivered the best overall performance, achieving the shortest scanning times and the highest trueness, while light-colored or geometrically complex SBs, such as ivory and MedentiWings, compromised both accuracy and efficiency. Additionally, deviations were more pronounced in the posterior regions, regardless of SB type.

These findings underscore the importance of carefully selecting SBs with favorable optical and geometric properties to optimize digital workflows and achieve predictable, high-quality prosthetic outcomes. The observed positive correlation between scanning time and RMS deviation further suggests that longer scanning procedures are associated with reduced trueness, highlighting the need for efficient scanning protocols.

In summary, informed selection of SBs is crucial for the success of digital impressions in implant-supported rehabilitations, directly influencing the predictability, efficiency, and clinical acceptability of final outcomes.

7. Bibliography

7. Bibliography

1. Rutkūnas V, Gedrimienė A, Al-Haj Husain N, Pletkus J, Barauskis D, Jegelevičius D, et al. Effect of additional reference objects on accuracy of five intraoral scanners in partially and completely edentulous jaws: an in vitro study. J Prosthet Dent. 2023;130(1):111–8.

2. Marques S, Ribeiro P, Falcão C, Lemos BF, Ríos-Carrasco B, Ríos-Santos JV, et al. Digital Impressions in Implant Dentistry: A Literature Review. Int J Environ Res Public Health [Internet]. 2021 Jan 24 [cited 2024 Oct 18];18(3):1020. Available from: https://www.mdpi.com/1660-4601/18/3/1020

3. Bader Eddin MB, Önöral Ö. Influence of splinting scan bodies or incorporating three-dimensionally printed scan aids on the trueness of complete arch digital scans. J Prosthet Dent. 2024;132(4):828.e1-828.e12.

4. Iturrate M, Eguiraun H, Etxaniz O, Solaberrieta E. Accuracy analysis of complete-arch digital scans in edentulous arches when using an auxiliary geometric device. J Prosthet Dent. 2019;121(3):447–54.

5. Rutkūnas V, Auškalnis L, Pletkus J. Intraoral scanners in implant prosthodontics. A narrative review. J Dent. 2024;148:105152.

6. Albanchez-González MI, Brinkmann JCB, Peláez-Rico J, López-Suárez C, Rodríguez-Alonso V, Suárez-García MJ. Accuracy of Digital Dental Implants Impression Taking with Intraoral Scanners Compared with Conventional Impression Techniques: A Systematic Review of In Vitro Studies. Int J Environ Res Public Health. 2022;19(4):2026.

7. Shaikh M, Lakha T, Kheur S, Qamri B, Kheur M. Do digital impressions have a greater accuracy for full-arch implant-supported reconstructions compared to conventional impressions? an in vitro study. Indian Prosthodont Soc. 2022;22(4):398–404.

8. Azevedo L, Marques T, Karasan D, Fehmer Vincent and Sailer I, Correia A, Gomez-Polo M. Effect of splinting scan bodies on the trueness of complete arch digital implant scans with 5 different intraoral scanners. J Prosthet Dent. 2024;132(1):204–10.

9. Meneghetti PC, Li J, Borella PS, Mendonça G, Burnett LH. Influence of scanbody design and intraoral scanner on the trueness of complete arch implant digital impressions: An in vitro study. Heboyan A, editor. PLoS One. 2023;18(12):e0295790.

10. Wan Q, Limpuangthip N, Hlaing NHMM, Hahn S, Lee JH, Lee SJ. Enhancing scanning accuracy of digital implant scans: a systematic review on application methods of scan bodies. J Prosthet Dent. 2024;132:898.e1-898.e9.

11. Nedelcu R, Olsson P, Thulin M, Nyström I, Thor A. In vivo trueness and precision of full-arch implant scans using intraoral scanners with three different acquisition protocols. J Dent. 2023;128:104308.

12. Cheng J, Zhang H, Liu H, Li J, Wang HL, Tao X. Accuracy of edentulous full-arch implant impression: an in vitro comparison between conventional impression, intraoral scan with and without splinting, and photogrammetry. Clin Oral Implants Res. 2024;35(5):560–72.

13. Alkadi L. A Comprehensive Review of Factors That Influence the Accuracy of Intraoral Scanners. Diagnostics. 2023;13(21):3291.

14. Zhang YJ, Qian SJ, Lai HC, Shi JY. Accuracy of photogrammetric imaging versus conventional impressions for complete arch implant-supported fixed dental prostheses: a comparative clinical study. J Prosthet Dent. 2023;130(2):212–8.

15. Joensahakij N, Serichetaphongse P, Chengprapakorn W. The accuracy of conventional versus digital (intraoral scanner or photogrammetry) impression techniques in full-arch implant-supported prostheses: a systematic review. Evid Based Dent. 2024;24:1–8.

16. Huang R, Liu Y, Huang B, Zhang C, Chen Z, Li Z. Improved scanning accuracy with newly designed scan bodies: an in vitro study comparing digital versus conventional impression techniques for complete-arch implant rehabilitation. Clin Oral Implants Res. 2020;31(7):625–33.

17. Zhang T, Yang B, Ge R, Zhang C, Zhang H, Wang Y. Effect of a Novel 'Scan Body' on the In Vitro Scanning Accuracy of Full-Arch Implant Impressions. Int Dent J. 2024 Aug 1;74(4):847–54.

18. Ma J, Zhang B, Song H, Wu D, Song T. Accuracy of digital implant impressions obtained using intraoral scanners: a systematic review and meta-analysis of in vivo studies. Int J Implant Dent. 2023 Dec 6;9(1).

19. Canullo L, Pesce P, Caponio VCA, Iacono R, Luciani FS, Raffone C, et al. Effect of auxiliary geometric devices on the accuracy of intraoral scans in full-arch implant-supported rehabilitations: an in vitro study. J Dent. 2024;145:104979.

20. Ali K, Alzaid AA, Suprono MS, Garbacea A, Savignano R, Kattadiyil MT. Evaluating the effects of splinting implant scan bodies intraorally on the trueness of complete arch digital scans: a clinical study. J Prosthet Dent. 2024;132(4):781.e1-781.e7.

21. Gómez-Polo M, Sallorenzo A, Cascos R, Ballesteros J, Barmak AB, Revilla-León M. Conventional and digital complete arch implant impression techniques: an in vitro study comparing accuracy. J Prosthet Dent. 2024 Oct 1;132(4):809–18.

22. Mizumoto RM, Yilmaz B, McGlumphy EA, Seidt J, Johnston WM. Accuracy of different digital scanning techniques and scan bodies for complete-arch implant-supported prostheses. J Prosthet Dent. 2020;123(1):96–104.

23. Gómez-Polo M, Barmak AB, Ortega R, Rutkunas V, Kois JC, Revilla-León M. Accuracy, scanning time, and patient satisfaction of stereophotogrammetry systems for acquiring 3D dental implant positions: a systematic review. Journal of Prosthodontics. 2023 Dec 1;32:208–24.

24. Azevedo L, Marques T, Karasan D, Fehmer V, Sailer I, Correia A, et al. Influence of Implant Scanbody Material and Intraoral Scanner on the Accuracy of Complete-Arch Digital Implant Impressions. Int J Prosthodont. 2023;37:575–82.

25. Spagopoulos D, Kaisarlis G, Spagopoulou F, Halazonetis DJ, Güth JF, Papazoglou E. In Vitro Trueness and Precision of Intraoral Scanners in a Four-Implant Complete-Arch Model. Dent J (Basel). 2023 Dec 5;11(1):1–10.

26. Revell G, Simon B, Mennito A, Evans ZP, Renne W, Ludlow M, et al. Evaluation of complete-arch implant scanning with 5 different intraoral scanners in terms of trueness and operator experience. J Prosthet Dent. 2022 Oct 1;128(4):632–8.

27. Pattamavilai S, Ongthiemsak C. Accuracy of intraoral scanners in different complete arch scan patterns. J Prosthet Dent. 2024;131(1):155–62.

28. Tasaka A, Uekubo Y, Mitsui T, Kasahara T, Takanashi T, Homma S, et al. Applying intraoral scanner to residual ridge in edentulous regions: in vitro evaluation of inter-operator validity to confirm trueness. BMC Oral Health. 2019;19(1):264–74.

29. Azevedo L, Laureti A, Marques T, Pitta J, Fehmer V, Pozzi A, et al. Effect of Horizontal and Vertical Intraoral Scan Bodies on the Trueness of Complete-Arch Digital Implant Impressions: A Comparative In Vitro Study With Six Implants. Clin Oral Implants Res. 2025 Jun 11;Epub ahead of print.

30. Amin S, Weber HP, Finkelman M, El Rafie K, Kudara Y, Papaspyridakos P. Digital vs. conventional full-arch implant impressions: a comparative study. Clin Oral Implants Res. 2017;28(11):1360–7.

31. Mangano FG, Hauschild U, Veronesi G, Imburgia M, Mangano C, Admakin O. Trueness and precision of 5 intraoral scanners in the impressions of single and multiple implants: A comparative in vitro study. BMC Oral Health. 2019;19(1).

32. Mangano FG, Admakin O, Bonacina M, Lerner H, Rutkunas V, Mangano C. Trueness of 12 intraoral scanners in the full-arch implant impression: A comparative in vitro study. BMC Oral Health. 2020;20(1):1–21.

33. Papaspyridakos P, Gallucci GO, Chen CJ, Hanssen S, Naert I, Vandenberghe B. Digital versus conventional implant impressions for edentulous patients: Accuracy outcomes. Clin Oral Implants Res. 2016;27(4):465–72.

34. Revilla-León M, Methani MM, Özcan M. Impact of the ambient light illuminance conditions on the shade matching capabilities of an intraoral scanner. Journal of Esthetic and Restorative Dentistry. 2021;33(6):906–12.

35. Agustín-Panadero R, Estada MIC, Alonso Pérez-Barquero J, Zubizarreta-Macho Á, Revilla-León M, Gómez-Polo M. Effect of relative humidity on the accuracy, scanning time, and number of photograms of dentate complete arch intraoral digital scans. J Prosthet Dent. 2023;133(3).

36. Revilla-León M, Gohil A, Barmak AB, Gómez-Polo M, Pérez-Barquero JA, Att W, et al. Influence of ambient temperature changes on intraoral scanning accuracy. J Prosthet Dent. 2023;130(5):755–60.

37. Revilla-León M, Kois DE, Kois JC. A guide for maximizing the accuracy of intraoral digital scans. Part 1: Operator factors. Journal of Esthetic and Restorative Dentistry. 2023;35(1):230–40.

38. Rutkūnas V, Kuleš D, Revilla-León M, Akulauskas M, Auškalnis L, Gendvilienė I. Full-Arch Digital Implant Impression Trueness: An in Vivo Study. Clin Oral Implants Res. 2025;36(5):640–9.

39. An H, Langas EE, Gill AS. Effect of scanning speed, scanning pattern, and tip size on the accuracy of intraoral digital scans. J Prosthet Dent. 2024 Jun 1;131(6):1160–7.

40. Tan M, Yee S, Wong K, Tan Y, Tan K. Comparison of Three-Dimensional Accuracy of Digital and Conventional Implant Impressions: Effect of Interimplant

Distance in an Edentulous Arch. Int J Oral Maxillofac Implants. 2019;34(2):366–80.

41. Cheng J, Zhang H, Liu H, Li J, Wang HL, Tao X. Accuracy of edentulous full-arch implant impression: An in vitro comparison between conventional impression, intraoral scan with and without splinting, and photogrammetry. Clin Oral Implants Res. 2024;35(5):560–72.

42. Abou-Ayash S, Schimmel M, Özcan M, Ozcelik B, Brägger U, Yilmaz B. Trueness and marginal fit of implant-supported complete-arch fixed prosthesis frameworks made of high-performance polymers and titanium: An explorative in-vitro study. J Dent. 2021 Oct 1;113:103784.

43. Lu Q, Zhu Y, Chen Y, Xu P, Liang Y, Chen T. Accuracy of a 3D printed custom resin crossbar for complete arch implant scanning: An in vitro and in vivo study. J Prosthet Dent. 2025 Apr 1;133(4).

44. Etxaniz O, Amezua X, Jauregi M, Solaberrieta E. Obtaining more accurate complete arch implant digital scans with the aid of a geometric pattern: A dental technique. J Prosthet Dent. 2025;133(2):370–5.

8. Attachments

8. Attachments

Table 7 Assessment of the normality of RMS distributions maximum and minimum deviations by SB type.

Normality Test							
	SB	Kolmogorov-Smirnov[a]			Shapiro-Wilk		
		Statistic	gl	Sig.	Statistic	gl	Sig.
Time	Metallic	,180	10	,200*	,900	10	,217
	Ivory	,154	10	,200*	,948	10	,646
	Blue	,218	10	,196	,926	10	,407
	Small Blue	,189	10	,200*	,936	10	,505
	Medentika	,129	10	,200*	,963	10	,817
Global average RMS	Metallic	,115	10	,200*	,989	10	,995
	Ivory	,237	10	,119	,913	10	,301
	Blue	,264	10	,047	,887	10	,158
	Small Blue	,265	10	,045	,860	10	,076
	Medentika	,161	10	,200*	,927	10	,421
Mean RMS position 46	Metallic	,278	10	,028	,898	10	,207
	Ivory	,176	10	,200*	,952	10	,692
	Blue	,199	10	,200*	,942	10	,579
	Small Blue	,310	10	,007	,853	10	,063
	Medentika	,246	10	,089	,867	10	,092
Mean RMS position 42	Metallic	,115	10	,200*	,989	10	,995
	Ivory	,237	10	,119	,913	10	,301
	Blue	,264	10	,047	,887	10	,158
	Small Blue	,265	10	,045	,860	10	,076
	Medentika	,161	10	,200*	,927	10	,421
Mean RMS position 36	Metallic	,140	10	,200*	,931	10	,457
	Ivory	,173	10	,200*	,938	10	,531
	Blue	,233	10	,131	,934	10	,486
	Small Blue	,248	10	,083	,902	10	,229
	Medentika	,183	10	,200*	,953	10	,701
Mean RMS position 32	Metallic	,185	10	,200*	,907	10	,258
	Ivory	,155	10	,200*	,958	10	,768

	Blue	,235	10	,124	,872	10	,106
	Small Blue	,252	10	,072	,915	10	,317
	Medentika	,448	10	,000	,496	10	,000
Minimum deviations	**Metallic**	,168	10	,200*	,915	10	,320
	Ivory	,133	10	,200*	,965	10	,841
	Blue	,147	10	,200*	,952	10	,689
	Small Blue	,297	10	,013	,776	10	,007
	Medentika	,242	10	,100	,843	10	,048
Maximum deavitions	**Metallic**	,160	10	,200*	,951	10	,675
	Ivory	,200	10	,200*	,943	10	,582
	Blue	,208	10	,200*	,926	10	,406
	Small Blue	,455	10	,000	,517	10	,000
	Medentika	,149	10	,200*	,957	10	,748
Minimum deviation position 46	**Metallic**	,251	10	,073	,883	10	,141
	Ivory	,140	10	,200*	,961	10	,802
	Blue	,147	10	,200*	,952	10	,689
	Small Blue	,297	10	,013	,776	10	,007
	Medentika	,143	10	,200*	,972	10	,908
Maximum deviation position 46	**Metallic**	,301	10	,011	,879	10	,128
	Ivory	,200	10	,200*	,943	10	,582
	Blue	,208	10	,200*	,926	10	,406
	Small Blue	,436	10	,000	,557	10	,000
	Medentika	,186	10	,200*	,964	10	,834
Minimum deviation position 42	**Metallic**	,168	10	,200*	,915	10	,320
	Ivory	,149	10	,200*	,977	10	,949
	Blue	,147	10	,200*	,952	10	,689
	Small Blue	,297	10	,013	,776	10	,007
	Medentika	,242	10	,100	,843	10	,048
Maximum deviation position 42	**Metallic**	,160	10	,200*	,951	10	,675
	Ivory	,200	10	,200*	,943	10	,582
	Blue	,208	10	,200*	,926	10	,406
	Small Blue	,193	10	,200*	,949	10	,661
	Medentika	,149	10	,200*	,957	10	,748
Minimum deviation position 36	**Metallic**	,456	10	,000	,531	10	,000
	Ivory	,124	10	,200*	,954	10	,710
	Blue	,168	10	,200*	,970	10	,887
	Small Blue	,207	10	,200*	,874	10	,112

	Medentika	,196	10	,200*	,965	10	,838
Maximum deviation position 36	**Metallic**	,150	10	,200*	,950	10	,666
	Ivory	,127	10	,200*	,959	10	,769
	Blue	,225	10	,163	,938	10	,534
	Small Blue	,261	10	,051	,903	10	,238
	Medentika	,168	10	,200*	,968	10	,872
Minimum deviation position 32	**Metallic**	,119	10	,200*	,986	10	,988
	Ivory	,133	10	,200*	,965	10	,845
	Blue	,142	10	,200*	,970	10	,889
	Small Blue	,247	10	,083	,825	10	,029
	Medentika	,490	10	,000	,438	10	,000
Maximum deviation position 32	**Metallic**	,145	10	,200*	,954	10	,711
	Ivory	,132	10	,200*	,920	10	,356
	Blue	,183	10	,200*	,902	10	,233
	Small Blue	,193	10	,200*	,950	10	,669
	Medentika	,418	10	,000	,539	10	,000
Mean RMS posterior region	**Metallic**	,152	10	,200*	,927	10	,415
	Ivory	,156	10	,200*	,909	10	,276
	Blue	,259	10	,056	,832	10	,036
	Small Blue	,253	10	,069	,853	10	,064
	Medentika	,182	10	,200*	,938	10	,528
Mean RMS anterior region	**Metallic**	,208	10	,200*	,948	10	,651
	Ivory	,158	10	,200*	,944	10	,602
	Blue	,212	10	,200*	,896	10	,196
	Small Blue	,161	10	,200*	,919	10	,351
	Medentika	,363	10	,001	,590	10	,000
Minimum deviation posterior region	**Metallic**	,339	10	,002	,697	10	,001
	Ivory	,146	10	,200*	,931	10	,459
	Blue	,239	10	,110	,945	10	,605
	Small Blue	,319	10	,005	,713	10	,001
	Medentika	,228	10	,151	,885	10	,149
Minimum deviation anterior region	**Metallic**	,156	10	,200*	,916	10	,323
	Ivory	,219	10	,191	,914	10	,308
	Blue	,211	10	,200*	,902	10	,232
	Small Blue	,223	10	,173	,840	10	,044
	Medentika	,453	10	,000	,497	10	,000
	Metallic	,149	10	,200*	,917	10	,336

Maximum deviation posterior region	**Ivory**	,213	10	,200*	,948	10	,640
	Blue	,242	10	,100	,915	10	,315
	Small Blue	,394	10	,000	,637	10	,000
	Medentika	,179	10	,200*	,964	10	,834
Maximum deviation anterior region	**Metallic**	,111	10	,200*	,936	10	,509
	Ivory	,125	10	,200*	,953	10	,699
	Blue	,256	10	,063	,810	10	,019
	Small Blue	,251	10	,075	,916	10	,327
	Medentika	,223	10	,175	,858	10	,072

***. This is a lower bound of the true significance level.**

a. Lilliefors Significance Correction